MISSOURI S&T

Missouri University of Science and Technology

Scholars' Mine

Materials Science and Engineering Faculty Research & Creative Works

Materials Science and Engineering

01 Jan 1995

Anomalous-diffusion Model of Ionic Transport in Oxide Glasses

David L. Sidebottom

Peter F. Green

Richard K. Brow
Missouri University of Science and Technology, brow@mst.edu

Follow this and additional works at: https://scholarsmine.mst.edu/matsci_eng_facwork

Part of the Materials Science and Engineering Commons

Anomalous-diffusion model of ionic transport in oxide glasses

D. L. Sidebottom, P. F. Green, and R. K. Brow

Department 1845, Sandia National Laboratories, Albuquerque, New Mexico 87185-0607

(Received 20 June 1994; revised manuscript received 12 September 1994)

The power-law frequency dependence of both the conductivity, $\sigma(\omega)$, and permittivity, $\varepsilon(\omega)$, of ion-conducting materials suggests that self-similar or scale-invariant behavior influences the transport of ions at high frequencies. Using an anomalous-diffusion model, we derive relevant power-law expressions for $\sigma(\omega)$ and $\varepsilon(\omega)$ and compare these with measurements performed on LiPO$_3$ glass. Superior fits to the measured data are obtained compared to the commonly used Kohlrausch-Williams-Watts (KWW) description of the electrical modulus, most particularly in the notorious high-frequency regime. Evaluation of our results in terms of an anomalous-diffusion model suggests the dominance of interaction-based constraints to diffusion.

I. INTRODUCTION

The electrical properties of ion-conducting glasses display frequency dependences that are, at present, still poorly understood.[1] The permittivity ε and the conductivity σ, real and imaginary parts of the complex dielectric constant $\varepsilon^* = \varepsilon - i\sigma/\omega$, exhibit power-law behavior. Power-law behavior is normally associated with systems that are either self-similar or possess scale invariances. Such systems exhibit identical behavior once appropriate rescaling is performed.[2]

Jonscher[3] observed that the behavior of $\sigma(\omega)$ for a variety of ion-conducting materials could be well described by an equation of the form

$$\sigma = \sigma_0 + A_\sigma \omega^n , \tag{1}$$

where $0.5 < n < 0.9$. This common behavior of a wide variety of dissimilar materials led Jonscher to describe Eq. (1) as the "universal" response. While σ_0 and A_σ merely establish the scales of the dc and ac conductivities, respectively, the exponent n is related to the nature of the physical process controlling the conduction of ions. Unlike situations of strict universality, where n is constant for all materials, the range of n observed by Jonscher suggests that n may vary among differing subclasses of materials. Thus, the response of n to variables such as temperature, ion concentration, and glass structure, should provide additional insight into the underlying physics. In this regard some recent studies have been presented. Lee, Liu, and Nowick,[4] for example, have shown that for the network forming glass, Na$_2$O/3SiO$_2$, n exhibits a temperature dependence and increases to a value of 1.0 as the temperature approaches zero Kelvin. This trend has also been more generally discussed by Angell.[5] With regard to glass structure, Kahnt[6] found that $\sigma(\omega)$ of a wide variety of structurally different ion-conducting glasses could be scaled so as to describe a common universal curve with $n \approx 0.67 \pm 0.03$. This provides strong evidence that scale invariances exist in ion-conducting glasses.

The dc part of the conductivity σ_0 appears to be reasonably well understood. It is currently thought to arise from the activated hopping of ions past local energy barriers. This is supported by the Arrhenius temperature dependence commonly exhibited by σ_0, and a number of theoretical efforts which have been successful in predicting the activation energies associated with the dc conductivity including early work by Anderson and Stuart[7] and more recent work by Elliot.[8] In these approaches, the energy barrier faced by the ion is decomposed into a Coulombic interaction between the ion and the network and a strain energy contribution. As a result, the motion of the ion is coupled with the mechanical dynamics of the host glass.[9]

The ac part of the conductivity remains an enigma. As the power-law feature is most prominent at high frequencies, it presumably must represent short-time motion that occurs prior to the hopping of the ion past its barrier; i.e., motion of the ion within its potential well, or possibly reiterative pairwise hopping between adjacent sites.[10]

Empirically, the ac part can be obtained by assuming that the response of the electric displacement D_e to increments of the electric field are described at short times by a Curie-von Schweidler[3] current

$$j(t) = dD_e/dt \approx t^{-n} . \tag{2}$$

There are currently two basic views on how this Curie-von Schweidler current arises. In the first, the high-frequency power law is assumed to represent the high-frequency wing of a relaxation process whose low-frequency wing is covered by dc conductivity.[11] This relaxation is presumed to result from hopping of ions over local energy barriers at high frequencies and long-range excursions over multiple barriers at low frequencies.

The second view interprets the frequency dependence of the conductivity as simply the result of changes in the manner in which the ions diffuse.[12] At long times (low frequency) the mean-square displacement of a diffusing ion is linear in time reflecting a constant coefficient of diffusion and hence also constant conductivity. At shorter times, the ion is strongly influenced by the local environment including interactions with other neighboring

    <u>51</u>   2770

ions, and exhibits a mean-squared displacement which increases more slowly.

In this spirit, a number of theoretical papers have recently proposed a model based upon anomalous diffusion to account for the ac part of the conductivity.[12-16] Numerical simulations for the mean-square displacement, $\langle r^2 \rangle$, of an ion performing a random walk on a fractal lattice indicate

$$\langle r^2 \rangle \propto \begin{cases} t^{1-n}, & 0 < n < 1 \; ; \quad r < \xi \\ t \; ; & r > \xi \end{cases} . \tag{3}$$

While a random walk on a fractal lattice is the traditional model for anomalous diffusion, more recent Monte Carlo simulations by Maass et al.[10] suggest that such diffusion can arise from Coulombic interactions in a disordered medium. Thus the actual presence of fractal structures does not appear to be a requirement.

The model appears to be of some general validity and has been successful at describing the dynamics of amorphous systems such as gels at the large length scales probed by light scattering[17] and polymers at the short length scales probed by neutron scattering.[18]

In this paper, we begin from Eq. (3) and derive expressions for $\varepsilon(\omega)$ and $\sigma(\omega)$. While the power-law forms obtained are not particularly new, our final expressions and related parameters involved can be traced back to physically relevant length and time scales involved in the diffusion process. In this sense, they provide a sound analytical approach to data reduction.

We compare our predictions with measurements performed on $LiPO_3$ as well as with data taken from the literature for which both $\sigma(\omega)$ and $\varepsilon(\omega)$ are available. Generally, the power-law fits are far superior to fits obtained by the more common electrical modulus formalism originated by Moynihan and co-workers,[19,20] as they are particularly successful at reproducing the much discussed high-frequency wing of $M''(\omega)$.

II. THEORY

We begin by considering a parallel plate capacitor with the material occupying the space between the plates. The magnitude of the displacement field that arises from an applied voltage across the plates is $D_e = \varepsilon^* E$, and for a parallel plate is equal to the charge density on the plates Q/A.[21] When a step voltage is applied causing E to increase from zero to some finite value E_0, the rate of change of D_e produces a current

$$\frac{dD_e}{dt} = \frac{d(Q/A)}{dt} = j(t) = \frac{d\varepsilon}{dt} E_0 . \tag{4}$$

Comparing Eq. (4) with the generalized form of Ohm's Law,

$$j(t) = \sigma(t) E_0 , \tag{5}$$

one arrives at the correspondence

$$\sigma = \frac{d\varepsilon}{dt} ,$$

or

$$\varepsilon = \int \sigma \, dt . \tag{6}$$

The conductivity can be obtained from the diffusivity by use of the Nernst-Einstein relation

$$\sigma = \frac{e^2 \rho_e}{k_B T} D , \tag{7}$$

and since

$$D = \frac{1}{6} \frac{d}{dt} \langle r^2 \rangle , \tag{8}$$

one finds from Eq. (6) that

$$\varepsilon = \frac{e^2 \rho_e}{6 k_B T} \langle r^2 \rangle = K \langle r^2 \rangle . \tag{9}$$

In an effort to maintain consistent units, we formalize Eq. (3) as

$$\langle r^2 \rangle = \begin{cases} R_0^2 (t/t_0)^{1-n} ; & r < \xi \\ \xi^2 (t/t_c) ; & r > \xi , \end{cases} \tag{10}$$

$$t_c = t_0 (\xi/R_0)^{2/(1-n)} , \tag{11}$$

where R_0 and t_0 are appropriate length and time scales for the discretized short-time motion, t_c is the time required to complete a mean-square displacement of ξ^2 and Eq. (11) follows from the boundary condition at $r = \xi$, and $t = t_c$. Introducing the reduced time $\tau = t/t_0$, Eq. (9) becomes

$$\varepsilon(\tau) = \begin{cases} A_1 \tau^{1-n} ; & \tau < \tau_c \\ A_2 \tau ; & \tau > \tau_c , \end{cases} \tag{12}$$

where $A_1 = K R_0^2$ and $A_2 = K \xi^2 (t_0/t_c)$.

Consider now the ratio A_1/A_2, which upon application of Eq. (11) becomes

$$A_1/A_2 = (t_c/t_0)^n . \tag{13}$$

Since a typical ratio of $t_c/t_0 \gg 1$ and $n > 0$, then $A_1 \gg A_2$, and we can parametrize Eq. (12) as

$$\varepsilon(\tau) = A_1 \tau^{1-n} + A_2 \tau , \tag{14}$$

which asymptotically behaves as Eq. (12) away from τ_c.

Following a related derivation by McCrum, Read, and Williams[22] based upon Boltzmann superposition, we can now use Eq. (14) to obtain $\varepsilon^*(\omega)$. Including the instantaneous polarization, ε_∞, that arises from distortions of the charges inside the medium, the response of D_e to an infinitesimal increase in the electric field is given by

$$dD_e = \varepsilon_\infty dE + dE [A_1 (\tau - u)^{1-n} + A_2 (\tau - u)] ,$$

or

$$D_e = \varepsilon_\infty E + A_1 \int_{-\infty}^{\tau} \frac{dE}{du} (\tau - u)^{1-n} du$$

$$+ A_2 \int_{-\infty}^{\tau} \frac{dE}{du} (\tau - u) du . \tag{15}$$

The electric field is assumed to be oscillatory so that

$$E(\tau)=E_e e^{i\Omega\tau} ,$$

where $\Omega=\omega t_0=\omega/\omega_0$, and upon integrating[22] Eq. (15) becomes

$$D_e/E \equiv \varepsilon^* = \varepsilon_\infty + A_1 g(n)\Omega^{n-1}\left[\sin\left[\frac{n\pi}{2}\right]-i\cos\left[\frac{n\pi}{2}\right]\right]$$
$$-iA_2/\Omega ,$$

or

$$\varepsilon=\varepsilon_\infty+A_1 g(n)\sin\left[\frac{n\pi}{2}\right]\Omega^{n-1} , \qquad (16a)$$

$$\sigma=\omega\varepsilon''=\omega_0 A_2+\omega_0 A_1 g(n)\cos\left[\frac{n\pi}{2}\right]\Omega^n , \qquad (16b)$$

where $g(n)=(1-n)\Gamma(1-n)=\Gamma(2-n)$.

Upon switching to a new frequency scale, $\Omega_c=\omega t_c=\omega/\omega_c$, introducing from comparison with Eq. (1), $\sigma_0=\omega_0 A_2$, and applying Eq. (13), these expressions become

$$\varepsilon=\varepsilon_\infty\left[1+\frac{(\sigma_0/\varepsilon_\infty)}{\omega_c}g(n)\sin\left[\frac{n\pi}{2}\right]\Omega_c^{n-1}\right] , \qquad (17a)$$

$$\sigma=\sigma_0\left[1+g(n)\cos\left[\frac{n\pi}{2}\right]\Omega_c^n\right] , \qquad (17b)$$

with

$$\sigma_0=K\xi^2\omega_c . \qquad (17c)$$

At this point the derivation is complete and results in two simultaneous expressions for both $\varepsilon(\omega)$ and $\sigma(\omega)$ involving a set of four parameters: σ_0, ε_∞, ω_c, and n. The first two of these parameters, σ_0 and ε_∞, establish the scale for the conductivity and permittivity, while the third, ω_c, establishes the frequency scale which separates the two regimes of diffusion.

In passing we wish to point out that these expressions can be further simplified by invoking the so-called Maxwell relation; i.e., that $\sigma_0/\varepsilon_\infty=\omega_\sigma$ is proportional to the crossover frequency ω_c.[5] Then Eqs. (17a) and (17b) simplify further to

$$\varepsilon=\varepsilon_\infty\left[1+h(n)\sin\left[\frac{n\pi}{2}\right](\omega/\omega_\sigma)^{n-1}\right] , \qquad (18a)$$

$$\sigma=\sigma_0\left[1+h(n)\cos\left[\frac{n\pi}{2}\right](\omega/\omega_\sigma)^n\right] , \qquad (18b)$$

with

$$h(n)=f^n g(n) ,$$

$$\omega_\sigma=f\omega_c .$$

While this simplification amounts to only a trivial substitution, it highlights the unique scale invariance that occurs. Only two parameters, σ_0 and ε_∞, are needed to establish the absolute scale of each function both along the ordinate as well as the abscissa. This ability to scale σ

and ε is a stringent requirement the measured data must meet.

Our final expressions for σ and ε involve a total of four fitting parameters (σ_0, ε_∞, ω_c, and n). This is one more than the more widely practiced method of data analysis involving the electrical modulus, $M^*(\omega)=1/\varepsilon^*(\omega)$ that was introduced by Macedo, Moynihan, and Bose.[19] The shape of $M^*(\omega)$ can be approximately fit using the Laplace transform of $d\phi_M/dt$ where

$$\phi_M(t)=\exp\left[-(t/\tau_m)^{\beta_m}\right] \qquad (19)$$

is the Kohlrausch-Williams-Watts (KWW) relaxation function. In addition, Ngai[11] has shown that this description of $M^*(\omega)$ results in a corresponding contribution to $\sigma(\omega)$ of the form

$$\sigma_{KWW}=B\exp(-E_a/k_B T)\omega^{1-\beta_m} , \qquad (20)$$

where E_a is the "primitive" activation energy.

While Eq. (19) can fit much of $M^*(\omega)$, it is widely acknowledged that the quality of the fit deteriorates severely at high frequencies,[5] precisely where the anomalous-diffusion mechanism is most active. While some argue that the shape of $M''(\omega)$ has "no significance relative to the motion of mobile ions",[23] others argue that the discrepancy between $M''(\omega)$ and the KWW fit arises from the presence of a second mechanism associated with ion motion along an asymmetric double-well potential (ADWP),[24] such that

$$\sigma_{ADWP}=CT^\alpha\omega , \quad \alpha\approx0.3\pm0.2 . \qquad (21)$$

The significance of this second contribution will be discussed in a later section.

The motivation for the KWW relaxation function is partly due to its overwhelming ability to describe a diversity of relaxation processes. This relaxation function is often interpreted as the result of several exponential relaxations, occurring in parallel, with a distribution of relaxation times. In this sense, the smallness of β_m is a measure of the breadth of that distribution. Thus τ_m and β_m together with ε_∞ are the three parameters required for fitting using the KWW relaxation.

While the present proposed fitting requires four parameters, σ_0 and ε_∞ are well-defined material properties and are easily found from the asymptotic behavior of σ and ε, respectively. Furthermore, the exponent n can be determined from σ_0 and ε_∞, independently of ω_c, by consideration of the ratio

$$\frac{\omega(\varepsilon-\varepsilon_\infty)}{\sigma-\sigma_0}=\tan\left[\frac{n\pi}{2}\right]=\text{const} , \qquad (22)$$

or from consideration of the ratio of ac and dc activation energies, given by

$$E_{ac}=-k_B T\ln A_\sigma=(1-n)E_{dc} . \qquad (23)$$

This last result has been emphasized in work by Almond and West[25] and shown by Dyre[23] to be a consequence of the scaling behavior often observed in $\sigma(\omega)$. It is also analogous to that proposed by Ngai[11] between the dc

conductivity and the "primitive" relaxation. These expressions thus aid in the determination of the parameters and serve to decrease the overall ambiguity of the fit.

III. EXPERIMENT

Lithium metaphosphate ($LiPO_3$) glass was made by melting mixtures of Li_2CO_3 and $NH_4H_2PO_4$ in platinum crucibles in air at 800 °C for 2 h and casting into ingots. Samples were annealed at 300 °C, then cooled to room temperature. The ingots were sectioned into square plates (3 cm × 3 cm × 1 mm) suitable for mounting into a custom-made impedance cell. These plates were reannealed at 300 °C and an approximately 1-cm² area on opposite faces was coated with Ag paint.

Measurements were performed in an environment of dry nitrogen. Two spring loaded contacts connected the Ag plates of the sample to the input ports of a commercial impedance analyzer (Schlumberger 1260) which together with a dedicated computer and software acquired measurements of the real and imaginary parts of the complex impedance of the material as a function of frequency between 1–10^6 Hz. Final calculations of σ and ε as well as M'' and M' were performed separately using the raw data and pertinent dimensions of the sample. Effects of electrode polarization[19] are clearly seen at low frequencies in $\sigma(\omega)$ and $\varepsilon(\omega)$, and we have omitted the data in these regimes when performing fits.

IV. RESULTS

Measurements of σ and ε at 34 °C over a range of frequencies from 1 to 10^6 Hz are reproduced in Fig. 1(a). At low frequencies, electrode polarization effects are witnessed, most notably in ε. A measurement of $\sigma(\omega)$ at −140 °C is shown for comparison with that at 34 °C in the inset to Fig. 1(a) and indicates a linear behavior consistent with the ADWP described by Eq. (21), but situated roughly a decade lower than the above-ambient spectra. Hence the contribution from the ADWP to the measured $\sigma(\omega)$ is negligible at the temperature and frequency range we have investigated. A more complete discussion of our subambient work is the subject of a forthcoming publication.[26]

$M''(\omega)$ and $M'(\omega)$ that result from σ and ε are plotted in Fig. 1(b). These display the usual features for M'' and M' as seen by others. In the M^* representation, electrode polarization effects are sharply suppressed at low frequencies. Included in the figure is a fit using the KWW approach [Eq. (19)] with $\beta_m = 0.60$. While this fit does reproduce the features of $M''(\omega)$ out to about 10^4 Hz, it severely underestimates the data at higher frequencies. Also included in both Figs. 1(a) and 1(b) are fits of Eqs. (17). Unlike the KWW fit, the power-law expressions reproduce the features of M'' and M' over the entire frequency range.

A series of measurements from 22 to 83 °C are shown in Figs. 2(a) and 2(b) using the modulus representation. We observe $\Gamma_m = 1.9 \pm 0.2$ decades implying $\beta_m \approx 0.58 \pm 0.05$ and constant with temperature. Fits of the power law are included and the parameters obtained
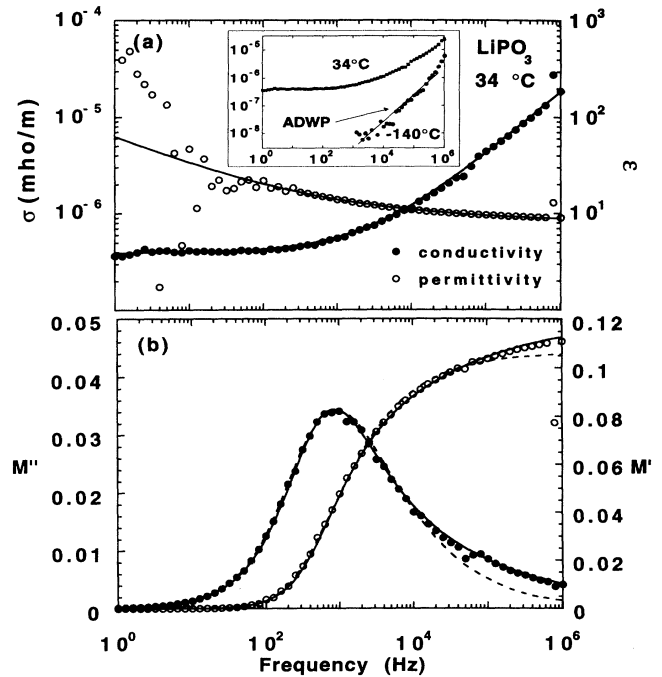

FIG. 1. (a) σ and ε at 34 °C. The lines are fits of Eqs. (17) with the parameters listed in Table I. Inset shows a comparison with the ADWP contribution observed at −140 °C. (b) Some data presented in the electrical modulus formalism. The dashed lines are fits of Eq. (19) for $\beta_m = 0.60$.
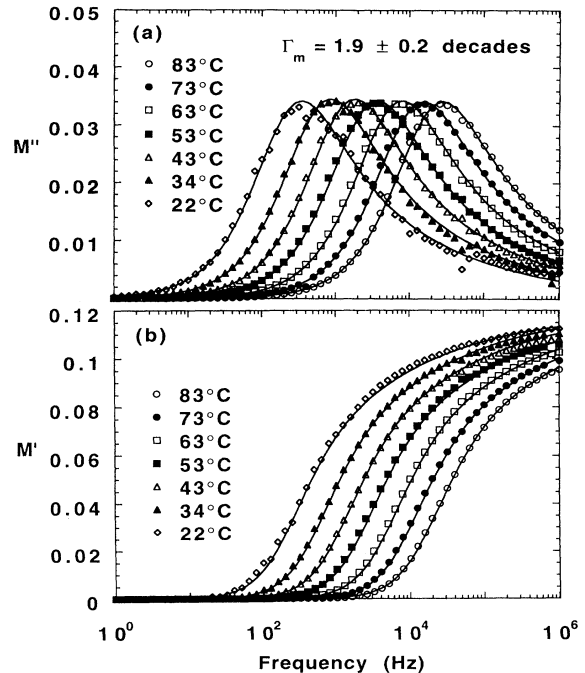

FIG. 2. (a) $M''(\omega)$ and (b) $M'(\omega)$ for temperatures between 22 and 83 °C. Solid lines are fits of Eqs. (17) with the parameters listed in Table I.

are listed in Table I. We observe that the exponent n is fairly constant at about 0.67 ± 0.03.

The value of n obtained from fits can also be compared with that which arises from plotting Eq. (22) versus frequency as shown for 34 °C in Fig. 3. Such a plot is constant over the frequency range of 10^2 to 10^6 Hz and from Eq. (22) this constant value results in $n = 0.66\pm0.03$ in excellent agreement with that obtained by fitting σ and ε.

In Fig. 4 we plot ω_σ vs $1/T$. Included are data beyond 83 °C, for which σ_0 could be determined but for which fits were not feasible due to ω_c increasing beyond 10^6 Hz, together with measurements of ω_σ by Martin.[27] These describe an Arrhenius behavior of the form

$$\omega_\sigma = fA_c \exp(-E_{dc}/k_B T) , \qquad (24)$$

with $E_{dc} = 0.66\pm0.02$ eV, and $A_c = 4\times10^{14}$ Hz. This prefactor is similar to that seen by others and is in the range of frequencies where infrared quasilattice vibrations of nonbridging oxygens (NBO's) and ions typically occur, as was discussed by Angell.[5]

Particularly important is the ability of Eqs. (17) to fit the high-frequency wing of M''. It has been widely acknowledged that fits using the KWW typically miss this wing and underestimate the actual data at these frequencies. The β_m of such fits can be estimated from the linewidth of M''.[19] From the measured linewidths we find $\beta_m \approx 0.58\pm0.05$ over the entire temperature range investigated. This value is, however, in strong conflict with that predicted by the coupling model[11] obtained from $\sigma(\omega)$ and described by Eq. (20), $\beta_m = 1-n = 0.33\pm0.05$. These β's represent linewidths of about 2 decades and 3.5 decades, respectively. This enormous difference is surprising for two accepted approaches to analyzing the same set of electrical data.[28]

The superiority of the power-law fit to describe the electrical properties of these ionic glasses as compared to that offered by the KWW is not isolated to LiPO₃ but can also be seen in previously published results for which an independent KWW fit has already been performed.

Measurements on $0.4Ca(NO_3)_2/0.6KNO_3$ in the melt and $Li_2O/Al_2O_3/2SiO_2$ in the glass published by Moynihan and co-workers[19,20] offer an excellent source for comparison. In addition to M' and M'', they also have provided σ and ε. Figures 5(a) and 6(a) show their data as taken from figures published in their paper together with fits by us using Eqs. (17). Figures 5(b) and 6(b) show the corresponding modulus of these data along with the same power-law fits used in Figs. 5(a) and 6(a) and the
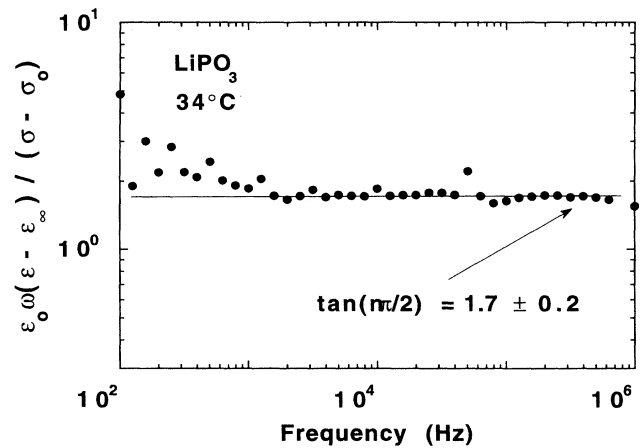

FIG. 3. Test of Eq. (22) at 34 °C. The line represents the constant behavior with $n = 0.66\pm0.03$.

KWW fit of Moynihan and co-workers. It is clearly evident, in spite of the errors introduced from transcribing the original data, that the power law provides an overall superior fit. This superiority is particularly evident at the high frequencies where the anomalous diffusion is most important.

While the superiority of the power-law fit stems partly from the additional parameter required, the parameter set itself is far from ambiguous, being composed of two well-defined material parameters $(\sigma_0, \varepsilon_\infty)$ and additional constraints such as that produced by Eqs. (22) and (23). Instead we argue that it is the difference in the physics that makes the fit superior. The KWW, while certainly a suitable empirical choice for constructing $M^*(\omega)$ rarely does the job properly. That it commonly cannot fit the high-frequency wing of M'' suggests that it fails to really describe the true physics behind ionic motion in these systems.

We find that Eqs. (17) provide an excellent description of the present experimental results. While one could

TABLE I. Results of fitting Eqs. (17).

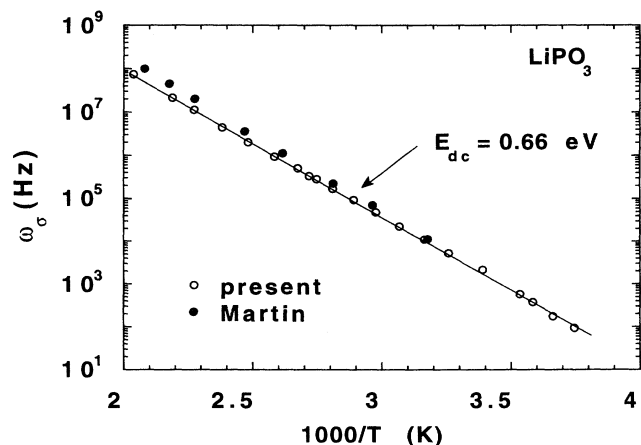| T (°C)	σ_0 (mho/m)	ε_∞	n	ω_c (Hz)
22	1.6×10^{-7}	8.4	0.67	2.6×10^3
34	3.9×10^{-7}	8.3	0.67	6.4×10^3
43	8.2×10^{-7}	8.3	0.67	1.3×10^4
53	1.7×10^{-6}	8.4	0.67	2.7×10^4
63	3.6×10^{-6}	8.4	0.67	5.8×10^4
73	7.0×10^{-6}	8.3	0.67	1.1×10^5
83	1.3×10^{-5}	8.3	0.67	2.1×10^5

FIG. 4. Arrhenius plot of ω_σ from the present study and from measurements by Martin (Ref. 27). The line is an Arrhenius fit with dc activation energy, $E_{dc} = 0.66\pm0.02$ eV.
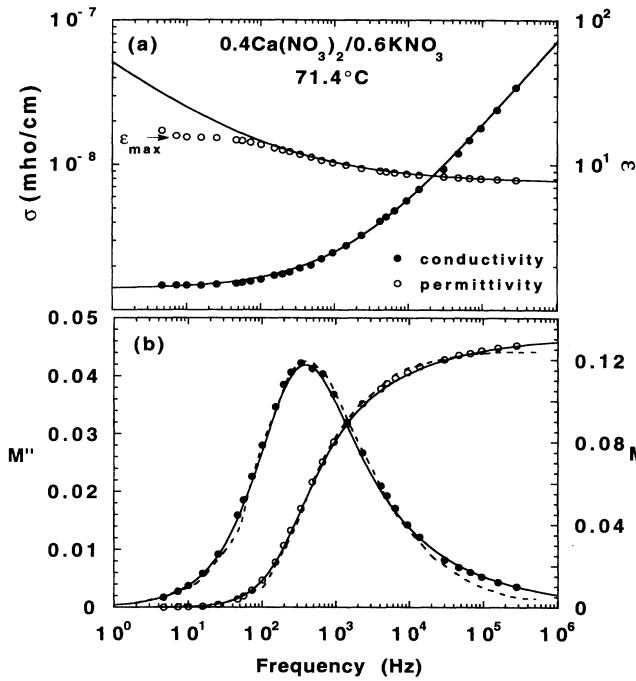
FIG. 5. Data from Macedo, Moynihan, and Bose (Ref. 19) for $0.4Ca(NO_3)_2/0.6KNO_3$ in both the (a) power-law and (b) electrical modulus representations. Solid lines are a fit of Eqs. (17) with $\sigma_0 = 1.5 \times 10^{-9}$, $\varepsilon_\infty = 7.7$, $n = 0.60$, $\omega_c = 3.3 \times 10^3$. Dashed line is a fit of the KWW [Eq. (19)] provided by Moynihan, Boesch, and Laberge (Ref. 20).
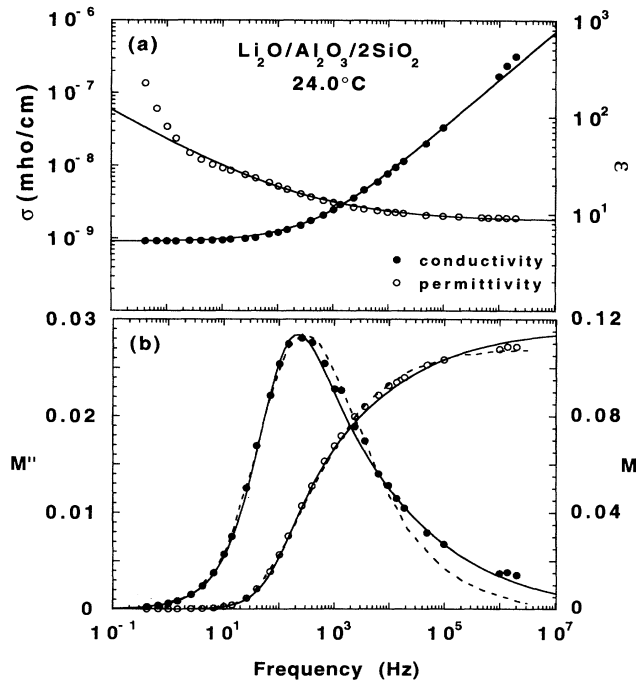

FIG. 6. Data from Macedo, Moynihan, and Bose (Ref. 19) for $Li_2O/Al_2O_3/2SiO_2$ in both the (a) power law and (b) electrical modulus representations. Solid lines are a fit of Eqs. (17) with $\sigma_0 = 9.1 \times 10^{-10}$, $\varepsilon_\infty = 8.9$, $n = 0.68$, $\omega_c = 7.9 \times 10^2$. Dashed line is a fit of the KWW [Eq. (19)] provided by Moynihan, Boesch, and Laberge (Ref. 20).

choose to view Eqs. (17) as merely a set of empirical relations involving σ_0, ε_∞, ω_c, and n, without any loss in describing the observed behavior, we now consider what these parameters convey about the anomalous-diffusion process and its scales.

First, using Eq. (17c) and the experimentally determined values $(\rho_e = 3 \times 10^{27}$ m$^{-3})$, we obtain $\xi \approx 1.4$ Å averaged over the temperature range investigated. This is well in accord with our expectations based upon ion hopping over local barriers associated with displacement to an adjacent site. Considering the paucity of *structure* available at such a small scale, it seems apparent that the walker must be influenced by *interactions* of a host of neighboring ions which also perform the same rapid wiggling.

Second, one generally finds that $\varepsilon(\omega)$ does not continue to rise as a power law as ω approaches 0, but instead would approach a constant value, $\varepsilon_{max} = \varepsilon_\infty + \Delta\varepsilon$, if not for the electrode polarization effects.[29] An example of this is shown in Fig. 5(a) where $\varepsilon_{max} \approx 16$. Our measurements at high temperatures also displayed such behavior with $\varepsilon_{max} \approx 18$. While not specifically accounted for in our model, this low frequency limiting permittivity can be understood by the following physical argument. The permittivity is limited by the maximum dipole moment that forms between a nonbridging oxygen (NBO) and the diffusing ion. As the ion diffuses, the moment increases, but when the ion passes beyond ξ, the ion has roughly moved into an adjacent site and now its dipole moment is associated to the new NBO. Thus the dipole moment passes through a maximum at $p_{max} = e(R_{NBO}/2)$ or roughly $p_{max} \approx e\xi$. Using, as a first approximation, the classical expression for the permittivity of a thermodynamic system of permanent but randomly oriented dipoles,[21] $\Delta\varepsilon = \rho_e p^2/3kT$, we estimate $\varepsilon_{max} \approx 21$ in accord with the measured result.

Last, we reflect upon the value of $n = 0.67$ observed. This value was commonly found in a recent literature survey we conducted[28] suggesting that it is a universal value. This particular value is in the range of that obtained at low temperatures in the Monte Carlo simulation by Maass et al.[10] This together with the small scale of ξ, tends to support the Coulombic interaction-based diffusion models such as the jump-relaxation model of Funke[12] and the Coulomb-interacting lattice gas model of Maass and co-workers.[10,14]

V. CONCLUSIONS

The conductivity and permittivity of ion-conducting glasses display power-law dependences on frequency. These power laws are found to conform to predictions of a model based upon the anomalous diffusion of ions at short lengths. Many in the past have used the more traditional data treatment based upon a KWW decay function used to describe the corresponding electrical modulus. This traditional approach commonly underestimates the data at high frequencies. We find, however, that the proposed power-law treatment provides a superior fit which is capable of describing both the $\sigma(\omega)$ and $\varepsilon(\omega)$ curves as well as $M'(\omega)$ and $M''(\omega)$ over the entire

range of frequencies [particularly the high-frequency wing of $M''(\omega)$].

It is also important to stress that the superiority of the power-law fit is a general result of the form of Eqs. (17). Although Eqs. (17) were derived beginning from anomalous-diffusion concepts, the basic starting point is embodied in the so-called Curie–von Schweidler current, $j(t) \approx t^{-n}$. These power laws are somewhat generic and can be interpreted as empirical functions of the parameters σ_0, ε_∞, and n as well as in terms of the anomalous-diffusion parameters. Either way, Eqs. (17) provide a superior description of the dielectrical properties of these ion-conducting glasses as compared with fits of KWW as described by Moynihan and Macedo.

However, should we choose to interpret our results for LiPO$_3$ in terms of anomalous-diffusion parameters ξ and n, the results clearly suggest that the anomalous diffusion originates from Coulombic interactions rather than from details of the structure. This is consistent with the findings of Kahnt,[6] and is apparent from the extremely small (substructural) size of ξ which indicates that the anomalous diffusion is limited to regions below about 2 Å.

ACKNOWLEDGMENTS

[1] A. Hunt, J. Non-Cryst. Solids **160**, 183 (1993).

[2] H. E. Stanley, *Introduction to Phase Transitions and Critical Phenomena* (Oxford University Press, Oxford, 1971).

[3] A. K. Johscher, Nature (London) **267**, 673 (1977).

[4] W. K. Lee, J. F. Liu, and A. S. Nowick, Phys. Rev. Lett. **67**, 1559 (1991).

[5] C. A. Angell, Chem. Rev. **90**, 523 (1990).

[6] H. Kahnt, Ber. Bunsenges. Phys. Chem. **95**, 1021 (1991).

[7] O. L. Anderson and D. A. Stuart, J. Am. Ceram. Soc. **37**, 573 (1954).

[8] S. R. Elliot, J. Non-Cryst. Solids **160**, 29 (1993).

[9] P. F. Green, D. L. Sidebottom, and R. K. Brow, J. Non-Cryst. Solids **172-174**, 1352 (1994).

[10] P. Maass, J. Petersen, A. Bunde, W. Dieterich, and H. E. Roman, Phys. Rev. Lett. **66**, 52 (1991),

[11] K. L. Ngai and O. Kannert, Solid State Ionics **53-56**, 936 (1992).

[12] K. Funke, Ber. Bunsenges. Phys. Chem. **95**, 955 (1991).

[13] M. Wagener and W. Schirmacher, Ber. Bunsenges. Phys. Chem. **95**, 983 (1991).

[14] A. Bunde and P. Maass, J. Non-Cryst. Solids **131-133**, 1022 (1991).

[15] G. A. Niklasson, J. Appl. Phys. **62**, R1 (1987).

[16] L. A. Dissado and R. M. Hill, J. Appl. Phys. **66**, 2511 (1989).

[17] S. Z. Ren, W. F. Shi, W. B. Zhang, and C. M. Sorensen, Phys. Rev. A **45**, 2416 (1992); S. Z. Ren and C. M. Sorensen, Phys. Rev. Lett. **70**, 1727 (1993).

[18] J. Colmenero, A. Alegria, A. Arbe, and B. Frick, Phys. Rev. Lett. **69**, 478 (1992).

[19] P. B. Macedo, C. T. Moynihan, and R. Bose, Phys. Chem. Glasses **13**, 171 (1972).

[20] C. T. Moynihan, L. P. Boesch, and N. L. Laberge, Phys. Chem. Glasses **14**, 122 (1973).

[21] J. D. Jackson, *Classical Electrodynamics* (Wiley, New York, 1975).

[22] N. G. McCrum, B. E. Read, and G. Williams, *Anelastic and Dielectric Effects in Polymeric Solids* (Dover, New York, 1991).

[23] J. C. Dyre, J. Non-Cryst. Solids **135**, 219 (1991).

[24] K. L. Ngai, U. Strom, and O. Kannert, Phys. Chem. Glasses **33**, 109 (1992).

[25] D. P. Almond, G. K. Duncan, and A. R. West, Solid State Ionics **8**, 159 (1983); D. P. Almond and A. R. West, *ibid.* **9&10**, 277 (1983).

[26] D. L. Sidebottom, P. F. Green, and R. K. Brow (unpublished).

[27] S. W. Martin, Ph.D. thesis, Purdue University, 1986.

[28] D. L. Sidebottom, P. F. Green, and R. K. Brow (unpublished).

[29] J. M. Hyde, M. Tomazawa, and M. Yoshiyagawa, Phys. Chem. Glasses **28**, 174 (1987).